

# Electroless Ni-Cr-B on Diamond Particles for Fabricated Copper/Diamond Composites as Heat Sink Materials

Z. Abdel Hamid<sup>\*1</sup>, F. Abdel Mouez<sup>1</sup>, F. A. Morsy<sup>2</sup> and N. A. khalifa<sup>2</sup>

<sup>a</sup>Central Metallurgical R & D Institute (CMRDI) Cairo, Egypt

<sup>b</sup>Faculty of Science, Chemistry department, Helwan University, Helwan, Egypt

<sup>\*1</sup>forzeinab@yahoo.com

## Abstract

The ideal thermal management materials working as heat sink should have a high thermal conductivity combined with low thermal expansion. To meet these market demands, copper/diamond composites were fabricated using electroless and powder metallurgical techniques. Comparison between conventional Cu/diamonds and Cu/Ni-Cr-B coated diamond composites has been investigated using different diamond percents. The results reveal that the produced Cu/Ni-Cr-B coated diamond composites with 20 Vf % diamond exhibit the well bonding between coated diamond and copper matrix. The properties of the composites materials using coated diamond were greater than those of the conventional Cu/diamond composites. On fracture surface of the composites, it was found that preferential adhesion between Cu and uncoated diamond occurs on the (100) face only of diamond, while good adhesion force between coated diamond and Cu matrix occurs on all faces of diamond.

## Keywords

*Powder Technology; Ceramic Composites; Deposition; Thin Films; Sintering ; Cu/Diamond Composite.*

## Introduction

Heat sink is a passive component that cools a device by dissipating heat into the surrounding air. The ideal material working as heat sink and heat spreader should have a low coefficient of thermal expansion (CTE) and high thermal conductivity. The most common heat sink materials are aluminum and copper alloys ( Kidalov SV, Shakhov FM 2009), (Moustafa SF et al.,1996), (Xingcun CT,2011) Additionally, Cu metal matrix composites (MMCs) such as Cu/Mo, Cu/W can be used as heat sink materials,( Ruch PW,2006). The use of diamond as a reinforcement materials in MMCs is thus very attractive, with the potential of both lowering the CTE of metal matrix into the CTE range of semiconductors and ceramic insulators. The

adhesion between metal matrix and diamond was found to depend strongly on the processing condition. It is known from former experiments that there is a very weak bonding between the received diamonds and the pure copper matrix in the consolidated composite. Many research investigators have tried to overcome the problems of non-wettability of ceramic powder (such as diamond) with metals to enhance the bonding at the interface. Some of these investigations suggested coating the powder with a wettable layer, which may be carbides, oxides or nitrides (Honjo K,1986). The most common and advanced coating layer is the carbides, as they produce a composite material with good electrical and mechanical properties. Coating of reinforcement particles with a material that is wetted by the metal matrix avoids any difficulty in the fabrication of metal matrix composite. In the present study, the diamond powders were electroless coated with chromium alloy and then transformed to chromium carbide by in-situ process. Chromium is believed to be a good promoter due to its abilities to improve copper thermal stability and to increase copper dispersion. The main objective of this work was to synthesize and characterize Cu/diamond composite materials by powder metallurgy and electroless techniques. Coating diamond particles by Ni-Cr-B using electroless technique have been mixed with copper matrix to fabricate Cu/diamond composites. Finally, the properties of Cu/coated diamond composites were compared with the same materials containing uncoated diamond and composite containing Cr powder as alloying element.

## Experimental

Within this work, three groups were prepared. The first used diamond particles admixing with copper powder, second included diamond admixing with

alloying element Cr and copper powders, while the third included coating diamond particles with Ni-Cr-B then admixing with copper powder.

### Materials

The investigated diamond powders with grain sizes 20–40  $\mu\text{m}$  type RVD were supplied by Polaris Diamond Powder Co., Ltd. Copper powder has been fabricated using electroless technique.

### Coating for Diamond Particles

Before the application of the coating process, the diamond surface must be treated and activated to improve the coating adhesion. This treatment was explained briefly elsewhere [6]. The chemical composition and the operating conditions to prepare the diamond coatings with Ni-Cr-B alloys were illustrated in Table 1.

TABLE 1: CHEMICAL COMPOSITION AND OPERATING CONDITIONS OF THE ELECTROLESS PLATING SOLUTION FOR NI-CR-B

Composition	Concentration, $\text{gL}^{-1}$	Operating conditions
Chromium acetate	40	Temperature, 85-90°C
Nickel acetate	6	pH value 4.5
sodium acetate	65	Time, 2hr
Dimethyl amine borane (DMAB)	3	
Ammonium oxalate	1	

### Fabrication of Composites

The mixing process for all composites was carried out using MIXER/MILL SPEX 8000M for 20 min. The copper mixed with different diamond contents (10-30V%), milling, compacting under 100 bar pressure then sintered at 900°C for 1 hr in reducing atmosphere.

### Characterizations

Scanning electron microscope (SEM) with energy dispersive X-ray spectroscopy (EDS) model JEOL, JSM-5410 was used to assess the surface morphology and the compositions, respectively. The phase identification was determined by X-ray diffraction. The boron content of the Ni-Cr-B film was determined by inductively coupled plasma-mass spectrometer (ICP-MS). The densities of the composites were measured according to MPIF Standards 42, using Archimedes rule. The electrical resistivity was measured using Omega CL 8400 micrometer device. The macrohardness was measured using Vicker's macrohardness Test type HPV 30A using load 5 kg for 15 s. The rupture test was performed according to MPIF Standard 41. Coefficient of Thermal Expansion (CTE) was measured with a Netzsch dilatometer model 402C push rod. The thermal conductivity was

calculated from electrical resistivity measurement using Wiedemann and Franz equation (Hamid ZA et al., 2011).

## Results and Discussion

### Electroless Coating of Diamond With Ni-Cr-B

The influence of DMAB concentrations on the deposited process has been investigated. Figure 1 shows diamond coated with Ni-Cr-B using different concentrations of DMAB in plating solution and operated at PH 4.5 and 30°C for 2 hrs. The image of Fig. 1a reveals that the coating on the diamond particles deposited from plating solution containing  $1\text{gL}^{-1}$  seems to be a batched precipitation. While with increasing DMAB concentration up to  $3\text{gL}^{-1}$ , the image shows that the coating is regular and the deposit becomes denser and notable (Fig 1b). Beyond  $3\text{gL}^{-1}$  DMAB concentration, the crystallinity of the deposit increased, which caused an increase in the growth rate of the crystal with the resulting large crystal; leading to increase in the formation of nodules on the surface (Fig. 1c). Therefore,  $3\text{gL}^{-1}$  DMAB concentration was used in subsequent experiments in this study.

The chemical composition of the diamond coated with electroless NiCrB from baths containing different concentrations of DMAB is illustrated in Fig. 1d. EDS analysis illustrated that the weight percent of Cr increased with increasing DMAB concentration and the analyses were uniformly distributed throughout the film. Such behavior can be ascribed to the increase in the deposition rate with increasing DMAB concentrations in the plating solutions.

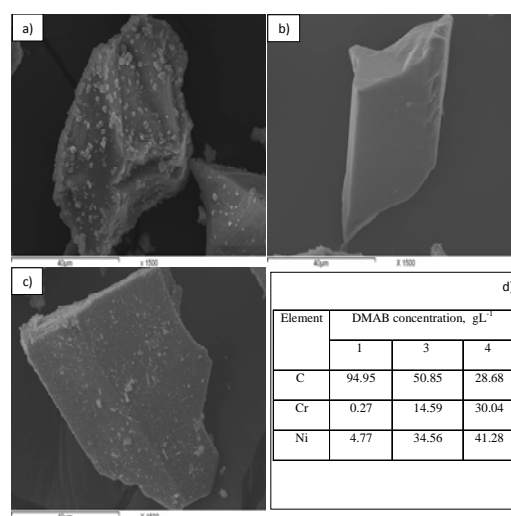
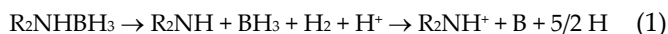
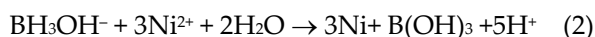


FIG. 1. SEM AND EDS OF THE DIAMOND COATED WITH NI-CR-B USING DIFFERENT CONCENTRATIONS OF DMAB IN PLATING SOLUTION AND OPERATED AT PH 4.5 FOR 2 HRS., A)  $1\text{gL}^{-1}$ , (B)  $3\text{gL}^{-1}$ , (C)  $4\text{gL}^{-1}$  AND D) EDS RESULTS.

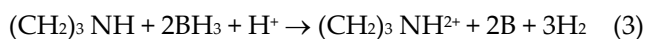
The mechanism of electroless deposition of metals is a complex process since it involves consecutive steps. The mechanism of electroless Ni-B has been studied by many investigators (Duhin A et al ,2009), (Mallory G.O ,1971) while the mechanism of formation of Ni-Cr-B remains unclear. Generally, aqueous solution of Cr is complex because it is exhibited in different oxidation states ( $\text{Cr}^{2+}$ ,  $\text{Cr}^{3+}$ ,  $\text{Cr}^{5+}$  and  $\text{Cr}^{6+}$ ). The reduction potential of  $\text{Cr}^{3+}$  is sufficiently lower (0.407 V) compared to other Cr ionic species (Lide DR,1995). It is possible to lower the reduction potential of metal ions by complexing it with suitable complexing agent. Ramesh et al. studied electroless plating of Cr-P alloy (Ramesh L et al,1996). Because the side reactions of electroless deposition, the overall utilization of reducing agent for reduction of  $\text{Cr}^{3+}$  to Cr is low even under the favorable conditions. This problem is minimized by using suitable complexing agent. Spectral studies of the plating bath solution revealed weak complexation of  $\text{Cr}^{3+}$  ions with sodium acetate which favored the electroless plating process. So, the mechanism of Ni-Cr-B coating remains unclear. In traditional Ni-B solution, the acid hydrolysis of DMAB occurs according to the following equations (Osaka T et al ,2003) :



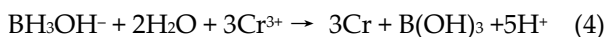
Most authors believe that the major species supplying electrons for metal-ion reduction is  $\text{BH}_3\text{OH}^-$ . Generally, DMAB has three active hydrogen atoms bonded to the boron, and theoretically should reduce three metal ions (such as Ni) for each ion of  $\text{BH}_3\text{OH}^-$ .



The boron reduction can be represented by the following reaction:



During electroless plating of Cr with DMAB as reducing agent, one could expect the following overall reaction similar to electroless nickel plating:



X-ray diffraction patterns for uncoated and coated diamond before and after heat-treatment are shown in Fig. 2. Figure 2a shows the peaks at  $2\theta$  44 and  $750^\circ$  attributed to the pure diamond, while XRD pattern for diamond coated with Ni-Cr-B (Fig. 2b) characterized by the amorphous structure as indicated by the broadening of the diffraction line. Figure 2c represents

XRD patterns of Ni-Cr-B after heat treatment at  $900^\circ\text{C}$  for 1 hr and reveals that Ni-Cr-B amorphous structure was converted to Cr,  $\text{BC}_2$ ,  $\text{Cr}_2\text{NiB}_6$  and Ni crystallite phases.

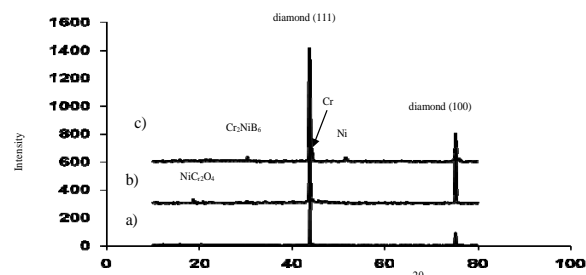


FIG. 2. XRD PATTERNS OF, A) UNCOATED DIAMOND, B) COATED DIAMOND WITH NI-CR-B BEFORE HEAT TREATMENT AND C) AFTER HEAT TREATMENT AT  $900^\circ\text{C}$  FOR 1 HR.

### Cu/diamond Composites

The surface morphologies of Cu/diamond Composites with different volume fraction diamond were observed by SEM. Figure 3 shows the morphologies of Cu/diamond composites containing 20 Vf% diamond. The porosity of the copper matrix was decreased compared with Cu/uncoated diamond or Cu/Cr-diamond composites. This may be attributed to the homogenous and high dense Cu-coating onto diamond particle, which caused the increasing compaction effect on the copper matrix that led to the decreasing porosity. A good adhesion between the matrix and the coated diamond led to lack of interfacial gap between the coated layer and the copper matrix that decreased the porosity (Ohsaki T et al. ,1977) (Caturla F et al.,1995) . The good wettability was related to the formation of carbide layer on the diamond surface. Since the uncoated diamond particles are easy to be stripped off during mechanical polishing, small pits are left on the surface of samples.

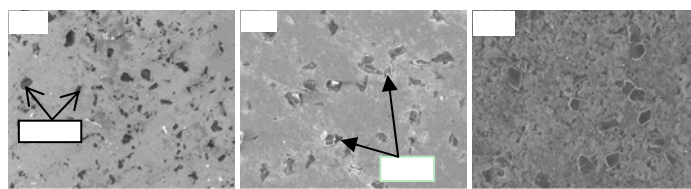


FIG. 3. SURFACE MORPHOLOGIES OF COMPOSITES CONTAINING 20VF% DIAMOND, A) CU/UNCOATED DIAMOND, B) CU/CR-UNCOATED DIAMOND AND C) CU/COATED DIAMOND COMPOSITES

### Characterizations of Cu/diamond Composites

Table 2 shows the relation between relative green densities of the different Cu/diamond composites with

different Vf%. It is clear that the relative green density depend strongly on the amount of diamond particles in the composite, and increases with increasing Vf% of diamond and attains the optimum value at 20 Vf%. This means that the densification is affected directly by diamond Vf%. The table reveals that the relative densities increased and the higher relative density was that of Cu/coated diamond.

Table 3 illustrates the electrical resistivity of the fabricated composites. It is clear that the electrical resistivity for all Cu composites decreased with increasing diamond Vf% up to 20Vf %, and Cu/coated diamond composite has the lowest electrical resistivity. Additionally, Table 3 shows macrohardness of the investigated composites. It is noticed that the hardness values of the Cu/coated diamond composite showed the highest hardness, followed by that of Cu/Cr mixed diamond, and the lowest hardness was registered for the Cu/uncoated diamond composites. The carbide layer has a very high hardness, and its presence improved the adhesion force between the diamond and the copper metal matrix, and at the same time it served as a barrier layer that transfers the strengthening effect of the diamond to the copper matrix (Khattab N .M,2001). The high hardness of carbide layers increases the effect of compaction pressure on Cu-matrix on one side and protects diamond from fragmentation on the other side.

TRS of the composites are listed also in Table 3. According to the data obtained, the TRS increased with the increasing diamond Vf % in the matrix and attained the optimum values at 20 Vf %. With further increase diamond Vf %, the TRS is slightly decreased. The copper Phase has plastically deformed to sharp edges. Diamond grains seem to be fractured mainly in the intergranular manner(Travitzky NA,1998). For the conventional method samples, it is clear that the

highest transverse rupture strength was recorded for composites of Cu/Cr mixed diamond compared with Cu/uncoated diamond. The Cu/Ni-Cr-B coated diamond composite has the highest TRS among all samples, which attributed to that the coated alloy acts as a barrier layer that decreases the pores at the interface and so gives a degree of adhesion that increases the strength of the final composite. All samples were bended and then partly fractured. This behavior could be attributed to the strengthened effect of the diamond reinforcement in the fabricated composite that resisted the fracture in the longitudinal direction. Additionally, the coated layer which consists of carbides and borides acts as crack propagation layer that transfers the strength of diamond to the copper matrix and also permits a good adhesion between the diamond and the copper matrix that gives more density and less porosity, consequently more strengthened composite.

Figure 4 shows the fracture surface of all investigated composites. Figure 4a illustrates the fracture surface of Cu/uncoated diamond composite. The image indicates poor bonding between diamond on (111) surfaces and Cu matrix and the adhered bonding on (100) diamond surface, which agrees with P.W. Ruch et al. (Ruch PW, 2006). Figure 4b illustrates the fracture surface of Cu/Cr-uncoated diamond composite. The image illustrates slightly improvment in Cu/diamond composite wettability. While, Fig.4c represents the fracture surface of the Cu/coated diamond composite and shows good wettability in the adhesion force of the interface layer between coated diamond and Cu matrix. The EDS of the interface layer proved the formation of the carbide layer which enhanced the adhesion force between diamond particle and Cu matrix.

TABLE (2): RELATION BETWEEN RELATIVE GREEN DENSITY AND THE RELATIVE DENSITY AFTER SINTERING VERSUS VOLUME PERCENT OF DIAMOND POWDERS

V <sub>f</sub> % of diamond	relative green density, %			The relative density after sintering, %		
	Cu/uncoated diamond	Cu/uncoated diamond + Cr	Cu/coated diamond Ni-Cr-B	Cu/uncoated diamond	Cu/uncoated diamond + Cr	Cu/coated diamond Ni-Cr-B
10	76	83	98	66.4	90	96.0
15	83	85	98	72	92	99.0
20	91	95	99	78	95	99.8
30	82	87	96	80	93	98.9

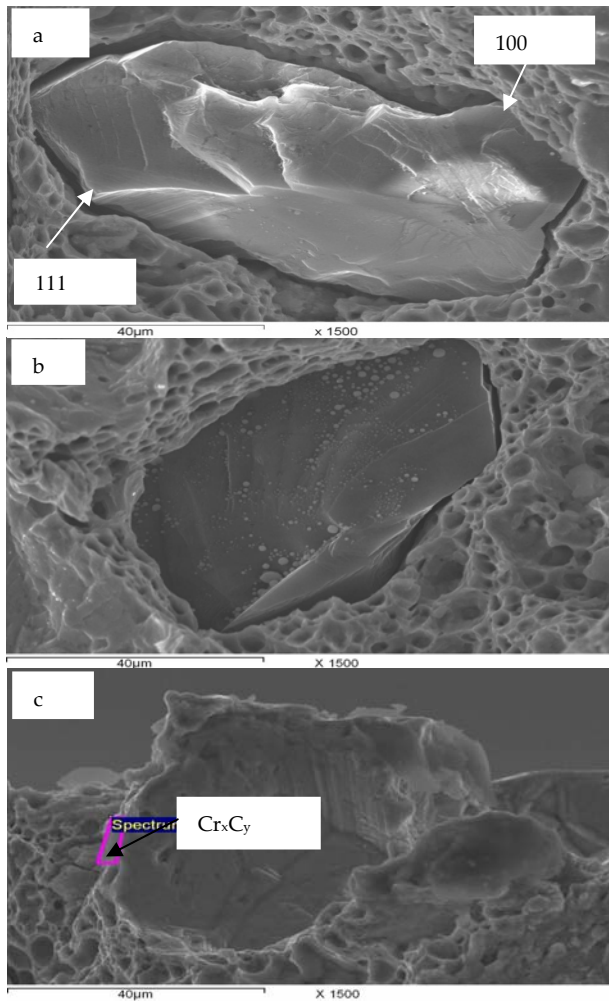


FIG. 4. SEM OF THE FRACTURE SURFACE FOR: A) CU/UNCOATED DIAMOND, B) CU/CR-UNCOATED DIAMOND, C) CU/NI-CR-B COATED DIAMOND.

Table 4 shows the variation of thermal conductivity and CTE of pure Cu and different composites with various Vf% diamond. It is clear that thermal conductivity increased from 352 for Cu/uncoated diamond composite to 450 Wmk<sup>-1</sup> for Cu/coated diamond composites at 20 Vf% diamond. The low thermal conductivity indicated a high thermal barrier resistance, no chemical affinity between copper and diamond; therefore, it is difficult to produce a bond of low thermal resistance and high mechanical strength between the matrix and the reinforcement. It can be

seen that the CTE of Cu/20 Vf% coated diamond composite decreases to 5×10<sup>-6</sup> K<sup>-1</sup>, which is about one-third of pure copper (17×10<sup>-6</sup> K<sup>-1</sup>).

TABLE 3: TRANSVERSE RUPTURE STRENGTH, VICKER MACROHARDNESS AND ELECTRICAL RESISTIVITY OF THE INVESTIGATED COMPOSITES

Investigate Composites	TRS, N/mm <sup>2</sup>	Hardness, Hv	Electrical resistivity, (μ Ω cm)
<b><u>Cu/ uncoated diamond</u></b>			
Cu/ 10 Vf% uncoated diamond	210	53	2.33
Cu/ 15 Vf% uncoated diamond	238	55	2.08
Cu/ 20 Vf% uncoated diamond	250	56	1.96
Cu/ 30 Vf% uncoated diamond	270	52	2.00
<b><u>Cu/ uncoated diamond with Cr mixed</u></b>			
Cu/ 10 Vf% diamond	698.86	55.00	1.81
Cu/ 15 Vf% diamond	750.00	58.38	1.80
Cu/ 20 Vf% diamond	852.61	67.18	1.78
Cu/ 30 Vf% diamond	618.29	59.13	1.79
<b><u>Cu/ coated diamond with Ni-Cr-B</u></b>			
Cu/ 10 Vf% coated diamond	1385.55	66.35	1.77
Cu/ 15 Vf% diamond	1789.69	77.04	1.76
Cu/ 20 Vf% diamond	1848.61	77.45	1.72
Cu/ 30 Vf% diamond	831.98	74.24	1.73

## Conclusions

- 1) Diamond powders can be coated with Cr-Ni-B by electroless technique.
- 2) The sintered materials made from coated powders exhibit homogeneity structure, low resistivity, porosity, and high densification, hardness and TRS properties.
- 3) Coating diamond promotes to produce a better coupling of matrix and reinforcement, thus leading to increase in thermal conductivities up to about 450 W/mK combined with low CTE (5 × 10<sup>-6</sup>/K).

TABLE 4: THERMAL CONDUCTIVITY AND COEFFICIENT OF THERMAL EXPANSION OF THE INVESTIGATED COMPOSITES

Investigate Composites	Thermal Conductivity (W/Mk)	CTE x10 <sup>-6</sup> K <sup>-1</sup>
Pure copper	352	17
Cu/ 20 Vf% uncoated diamond	378	10
Cu/ 20 Vf% uncoated diamond with Cr mixed	411	6
Cu/ 20 Vf% Ni-Cr-B coated diamond	450	5

## REFERENCES

- Caturla F, Molina F, Molina-Sabio M, and Rodriguez-Reinoso F. J., *Electrochem. Soc.*, 142 (1995) 4084-4090.
- Duhin A, Sverdlov Y, Feldman Y, and Shacham-Diamand Y., *Electrochimica Acta*, 54 (2009) 6036-6041.
- Hamid ZA, Moustafa SF, Morsy FA, Abdel Atty N, Abdel Mouez F., *Natural Science* 3 (2011) 936-947.
- Honjo K., Shindo A., *J. Mater. Sci.* 21 (1986) 2043
- Khattab N .M .M., Ph.D. Thesis, Dep. of Chem., Faculty of Girls, Ain Shams Univ., Cairo, Egypt, (2001).
- Kidalov SV, Shakhov F.M, *Materials*, 2 (2009) 2467-2495.
- Lide DR., "Hand Book of Chemistry and Physics", 76th ed., CRC Press, Boca Raton, FL, 1995–1996.
- Mallory G.O., *Plating*, 58 (1971) 319-322.
- Moustafa S.F, Moustafa M.A, El-Sahat O.A, *Mater. Lett.*, 29 (1996) 37-44.
- Ohsaki T, Yoshida M, Fukube Y and Nakamur K., *Thin Solid Films*, 45 (1977) 563-568.
- Osaka T, Takano N, Kurokawa T, Kaneko T and Ueno K., Ueno, *Surf. and Coat. Technol.*, 169-170 (2003) 124-127.
- Ramesh L., Sheshadri B.S., Mayanna S.M., *Trans. IMF* 74 (1996) 66 -72.
- Ruch P.W, Beffort O, Kleiner S, Weber L, Uggowitzer P.J., *Compos. Sci. Technol*, 66 (2006) 2677–2685.
- Travitzky N.A., *Materials letters* 36 (1998) 114-117.
- Xingcun C.T, *Advanced Materials for Thermal Management of Electronic Packaging*, Springer Series in Advanced Microelectronics, 30 (2011) 1-58.